

A new laser non-contact method for the measurement of spindle error motion

Charles Wang
Optodyne Inc.
1180 mahalo place
Compton, Ca.

Abstract

For accurate machining, the spindle error motion may cause inaccurate and poor finished parts, even with high volumetric positioning and dynamic contouring accuracy. Conventional measurement techniques using a precision spindle tester, capacitor transducers and an oscilloscope are very complex and heavy. Described here is a new laser non-contact method for the measurement of spindle error motion. The accuracy and resolution are high, the range is large, and there is no need for a heavy precision spindle tester. It is cost effective and saves time. Furthermore, to simplify the measurement, a single-direction measurement can be used to generate the polar plot without the need to measure both x- and y-directions simultaneously.

I. Introduction

In today's manufacturing world, high-speed machine tools with high feed rate and high-speed spindle are frequently required to deliver accuracy in the order of a few micrometers [1]. To achieve the high accuracy, both the static volumetric positioning errors [2,3] and the dynamic contouring errors [4] should be measured and maintained to within a few micrometers. Furthermore, the spindle error motion [5,6,7] should also be measured and maintained to within the allowed error budget.

Briefly, the major spindle error motion is caused by the alignment of the spindle rotational axis, the centerline of the tool holder and the centerline of the tool. All of these should be coaxial. Any deviation from coaxial will generate eccentric error motion. Other causes of the radial and axial error motions are the spindle bearings, structure error motion, etc [5].

Conventional measurement techniques using a precision spindle tester, capacitor transducers and an oscilloscope are complex and heavy [5,6,7]. The precision spindle tester is very heavy and need periodic calibration. The capacitor transducers are limited by the sensitivity, range and non-linearity.

Described here is a new laser non-contact method for the measurement of spindle error motion. The accuracy and resolution are high, the range is large, and there is no need for a heavy precision spindle tester. Since the laser system is used for the measurement of the static volumetric positioning accuracy [3] and the dynamic contouring accuracy [4], with some simple accessories and data analysis software, it can be used for the measurement of spindle error motion. The additional cost of the accessories and the software is rather low. Hence it is cost effective and saves time. Furthermore, the heavy precision tester is no longer needed.

As compared with conventional techniques, the advantages of the laser measurement method are: 1, higher accuracy and resolution, 2, larger standoff distance, 3, easy setup and operation, 4, no need for a heavy precision tester and periodical calibration, and 5, save cost and time.

II. Non-contact laser measurement

The unique property of the LDDM is the single aperture optical arrangement [8], that is, both the output laser beam and the receiving laser beam share the same aperture. Because of this single aperture optical arrangement, it is possible to use a flat surface reflector as the target such as a polished surface of a sphere. To increase the return signal, a focus lens is used to focus the laser beam at the surface of the sphere. A schematic showing the two lasers setup and the optical arrangement is shown in Fig. 1.

The hardware used for the test is an MCV-500-2 laser calibration system including two laser heads with focus lens, a precision sphere tester with adjustable center as the target, 2 PC interface cards, and a notebook PC with Windows™ software. A photo of the setup is shown in Fig. 2. The laser system accuracy is 1 ppm, the resolution is 0.01 μm, and the maximum data rate is 1000 data/sec.

One laser head is pointing in the x-direction and another laser head is pointing in the y-direction. As shown in Fig. 3, first align the sphere to the center of rotation by adjusting the 4 fine thread screws and make sure there are no changes in the laser readings or the readings are varied less than the background noise or vibration. Then rotate the tool holder together with the sphere tester 180 degrees. As shown in Fig. 4, after rotating the tool holder together with the sphere tester 180 degrees, the offset is twice the offset between the spindle axis of rotation and the tool centerline. Manually rotate the spindle from X to -X and from Y to -Y. The maximum difference in X direction is ΔX_M and in Y direction is ΔY_M . The offset between the spindle axis of rotation and the tool center Δ can be determined by

$$\Delta = 0.25 * \text{SQRT}[\Delta X_M * \Delta X_M + \Delta Y_M * \Delta Y_M], \quad \text{Eq. 1}$$

$$\varphi = \text{Arctan} [\Delta Y_M / \Delta X_M]. \quad \text{Eq. 2}$$

The accuracy of this measurement is limited by the roundness of the sphere, typically 0.5 μm. To measure the total spindle error motion, rotate the spindle and record the two laser systems readings, $\Delta X(t)$ and $\Delta Y(t)$, over several revolutions.

III. Basic theory

The total spindle error motion at a constant rotational speed can be expressed as a function of the angle θ and the number of cycles i .

$$r_i(\theta) = r_f + dr(\theta) + dr_i(\theta), \quad i = 1, 2, 3, \dots, N \quad \text{Eq. 3}$$

where r_f is the fundamental error motion, $dr(\theta)$ is the residual error motion, $dr_i(\theta)$ is the asynchronous error motion, θ is the rotational angle, and N is the total number of cycles [6].

Here r_f is due to the offset between the spindle axis of rotation and the center of the tool, $dr(\theta)$ is due to the spindle bearing, the non-roundness of the sphere, and other synchronous error motion, and $dr_i(\theta)$ is due to the structure error motion or other asynchronous error motion. Once the total spindle error motion $r_i(\theta)$ is measured, the r_f , $dr(\theta)$, $dr_i(\theta)$ can be determined by the following relations.

$$r_f = \langle \langle r_i(\theta) \rangle_i \rangle_\theta \quad \text{Eq. 4}$$

$$dr(\theta) = \langle r_i(\theta) \rangle_i - r_f \quad \text{Eq. 5}$$

where $\langle \rangle_i = \sum_i []/N$ is the average over N cycles and $\langle \rangle_\theta = \sum_\theta []/2\pi$ is the average over 2π angle.

Based on Ref. 6 and 7, the error motion values are defined as the followings.

Total error motion value = $\text{Max}_{i,\theta} \{ r_i(\theta) \} - \text{Min}_{i,\theta} \{ r_i(\theta) \}$

Average error motion value = $\text{Max}_\theta \{ r_f + dr(\theta) \} - \text{Min}_\theta \{ r_f + dr(\theta) \}$

Fundamental error motion value = r_f

Residual error motion value = $\text{Max}_\theta \{ dr(\theta) \} - \text{Min}_\theta \{ dr(\theta) \}$

Asynchronous error motion value = $\text{Max}_\theta \{ \text{Max}_i [r_i(\theta)] - \text{Min}_i [r_i(\theta)] \}$,

where $\text{Max}_i []$ is the maximum value over N cycles, $\text{Min}_i []$ is the minimum value over N cycles, $\text{Max}_\theta \{ \}$ is the maximum value over angles θ , and $\text{Min}_\theta \{ \}$ is the minimum value over angles θ .

For machine tool applications [7], there is a sensitive direction of spindle motion, defined as that component of axis motion that occurs in a direction that is directly toward or away from a cutting tool. There are two types of sensitive directions, one is the fixed sensitive direction, in which the work-piece is rotated by the spindle and the point of machining is fixed such as a lathe. The other is the rotating sensitive direction, in which the work-piece is fixed and the point of machining rotates with the spindle such as a milling machine [6].

There are 6 degrees of spindle error motion. However, as discussed in Ref [6] only three of them are relevant. These are the radial error motion, tilt error motion and axial error motion. The radial error motion is the error motion in a direction normal to the z-axis. The tilt error motion is the error motion in an angular direction relative to the z-axis. The axial error motion is the error motion co-linear with the z-axis.

Let the laser measurement in the x-direction be $\Delta X(\theta)$ and in the y-direction be $\Delta Y(\theta)$. For a fixed sensitive direction along the x-axis, the radial motion polar plot has the equation [6]

$$r(\theta) = r_0 + \Delta X(\theta) \quad \text{Eq. 6}$$

where r_0 is the base circle radius. For a rotating sensitive direction the radial motion is given by the equation [6]

$$r(\theta) = r_0 + \Delta X(\theta) \cos\theta + \Delta Y(\theta) \sin\theta \quad \text{Eq. 7}$$

In the analysis here, let the laser measurement in the x and y direction be

$$\Delta X(\theta) = A \cos\theta + u(\theta) \quad \text{Eq. 8}$$

$$\Delta Y(\theta) = A \sin\theta + v(\theta) \quad \text{Eq. 9}$$

where A is the offset between spindle axis of rotation and the center of the sphere, $u(\theta)$ and $v(\theta)$ are the error motion in the x- and y-direction respectively. Assume $u(\theta)$ and $v(\theta)$ are much smaller than A, the radial error motion can be expressed as

$$r(\theta) = \text{SQRT}[\Delta X(\theta)^2 + \Delta Y(\theta)^2] \quad \text{Eq. 10}$$

$$= A + u(\theta)\cos\theta + v(\theta)\sin\theta \quad \text{Eq. 11}$$

This is similar to Eq. 7. For the fixed sensitive direction, the radial error motion can be expressed as

$$r(\theta) = \Delta X(\theta) \quad \text{Eq. 12}$$

$$= A \cos\theta + u(\theta) \quad \text{Eq. 13}$$

To simplify the calculation, it is plausible to assume that the spindle error motion is axial symmetric. That is, the error motion measured in the x-direction is the same as measured in the y-direction shifted by 90 degree. Hence

$$\Delta X(\theta) = A \cos\theta + u(\theta) \quad \text{Eq. 8}$$

$$\Delta Y(\theta) = A \cos(\theta - \pi/2) + u(\theta - \pi/2) \quad \text{Eq. 14}$$

$$= A \sin\theta + v(\theta) \quad \text{Eq. 9}$$

where $v(\theta) = u(\theta - \pi/2)$ is a good approximation.

Hence, the radial error motion can be obtained by a laser measurement in the x-direction along.

For the tilt measurement, repeat the radial error motion measurement at a different height L. The tilt $\alpha(\theta)$ can be expressed as [6]

$$\alpha(\theta) = [r(\theta) \text{ at } L - r(\theta) \text{ at zero}] / L \quad \text{Eq. 15}$$

For axial error motion, use a mirror to bend the laser beam upward and point the focus of the laser beam to the center of rotation. The measured laser displacement in the z-direction is the axial error motion $Z(\theta)$.

IV. Test results and analysis

In the following analysis, data was collected on a CNC milling machine, spindle rotations were at 50 rpm to 1000 rpm, the sample rates were 60 to 1000 data/sec. First the sphere is aligned to the spindle axis of rotation. The maximum variation in x-direction and y-direction were less than 0.5 μm , which is limited by the non-roundness of the sphere. At the spindle rotation speed of 100 rpm and the sampling rate at 125 data/sec, the measured data in the x-direction are plotted in Fig. 5. It is clear that most of the asynchronous error motion is caused by the structure error motion and the non-roundness of the sphere. Fig. 6 is the measured data in the x-direction and at 1000 data/sec while the spindle rotational speed was at 800 rpm stopped and started again and stopped again. It is interesting to note that during stopping and starting the error motion increased 4 times.

Then the tool holder together with the tester was rotated 180 degree. The measured maximum deviation in x- and y-direction are 17 μm and 13 μm respectively. Hence the offset calculated by Eqs. 1 and 2 is 21.4 μm at an angle $\varphi = 37.4$ degree. At the spindle rotation speed of 100 rpm and at a data rate of 125 data/sec, the measured data in the x- and y-direction are plotted in Fig. 7 a and b, and the polar plot is plotted in Fig. 8. The average, maximum and minimum error motion is plotted in Fig. 9. Here the polar plot is broken open and plotted from $-\pi$ to π with magnified scale. Based on Eqs. 3, 4 and 5, the calculated fundamental error motion value is 0.005471 mm, the average error motion value is 0.001027 mm, and the asynchronous error motion value is 0.001633 mm.

To verify Eq. 14, a polar plot using the data in Fig. 7a as x and shifted 90 degree as y is shown in Fig. 10. The average, maximum and minimum error motion is plotted in Fig. 11. The calculated fundamental error motion value is 0.005503 mm, the average error motion value is 0.000968 mm, and the asynchronous error motion value is 0.001618 mm. Here, the differences between Figs. 9 and 11 are very small. Hence it is a good approximation to use Eq. 14 in place of Eq. 9. Hence a single direction measurement can be used to generate the radial error motion polar plot.

V. Summary and conclusion

In summary, we have described the new laser non-contact method for the measurement of spindle error motion. As compared with conventional techniques, the advantages of the laser measurement method are high accuracy, high resolution, large standoff distance, easy setup and operation, and no need for a heavy precision tester. Furthermore, a single-direction measurement can be used to generate the polar plot without the need to measure both x- and y-direction simultaneously.

Acknowledgements

Helpful discussions with members of the ASME B5/TC52 committee, particularly, D. Lovett, and D. Martin are acknowledged.

References

1. M. Omari, "Machine dynamics accuracy for automotive die manufacturing", Proceedings of the Second International Advanced Technology for Die and Mold Manufacturing Conference, Oct 16, 1997.
2. Charles Wang, "Laser vector measurement technique for the determination and compensation of volumetric positioning errors. Part I: basic theory", Review of Scientific Instruments, Vol. 71, No. 10, pp3933-3937, Oct 2000.
3. John Janeczko, Bob Griffin, and Charles Wang, "Laser vector measurement technique for the determination and compensation of volumetric positioning errors. Part II: experimental verification", Review of Scientific Instruments, Vol. 71, No. 10, pp3938-3941, Oct 2000.
4. Charles Wang and Bob Griffin, "A non-contact laser technique for the circular contouring accuracy measurement", Review of Scientific Instruments, Vol. 72, No. 2, February 2001.
5. J. Bryan, R. Clonser and E. Holland, "Spindle accuracy", American Machinist, Dec. 4, 1967.
6. Axes of rotation, methods for specifying and testing, An American National Standard, ASME B89.3.4M-1985 by the American Society of Mechanical Engineers, 1985.
7. Methods for performance evaluation of computer numerically controlled machining centers, An American National Standard, ASME B5.54-1992 by the American Society of Mechanical Engineers, 1992.
8. LDDM MCV-500 User's Guide, Optodyne, Compton, Ca (1999).

Figure captions

1. A schematic of laser systems and the sphere target.
2. A photo of a typical setup for the measurement of spindle error motion.
3. A schematic of the spindle, the tool holder, and the sphere tester.
4. A schematic illustrating the effect of rotating the tool holder by 180 degrees.
5. Spindle error motion measured in x-direction.
6. Spindle error motion measured in x-direction at 800 rpm with start and stop.
7. Spindle error motion measured in a, x-direction and b, y-direction, after the tool holder was rotated 180 degree.
8. A polar plot of the radial error motion after the tool holder was rotated 180 degree.
9. A plot of the average, maximum and minimum error motion.
10. A polar plot using the measurement in the x-direction and shifted 90 degrees for the y-direction.
11. A plot of the average, maximum and minimum error motion using the measurement in the x-direction and shifted 90 degrees for the y-direction.

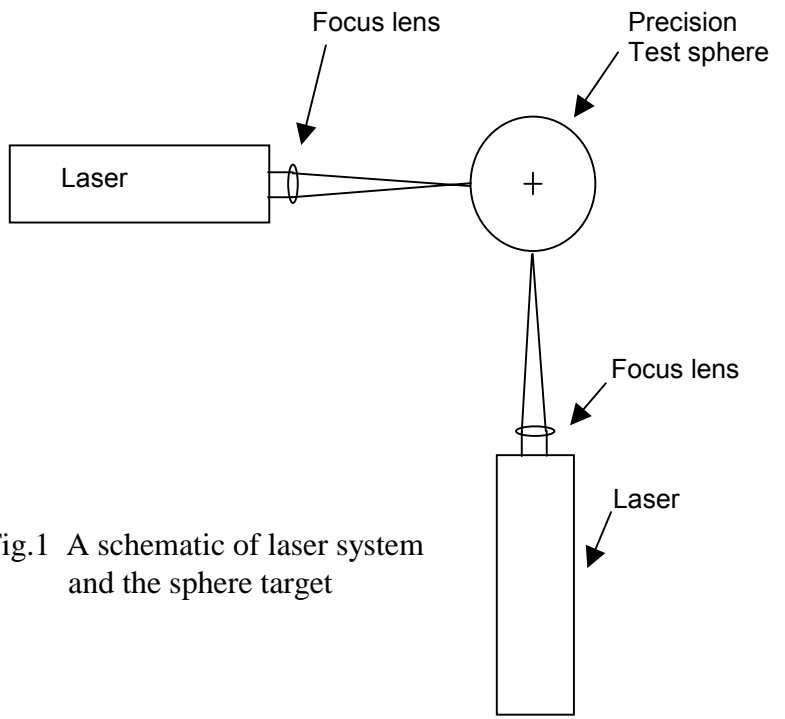


Fig.1 A schematic of laser system and the sphere target



Fig.2 A photo of a typical setup for the measurement of spindle error motion

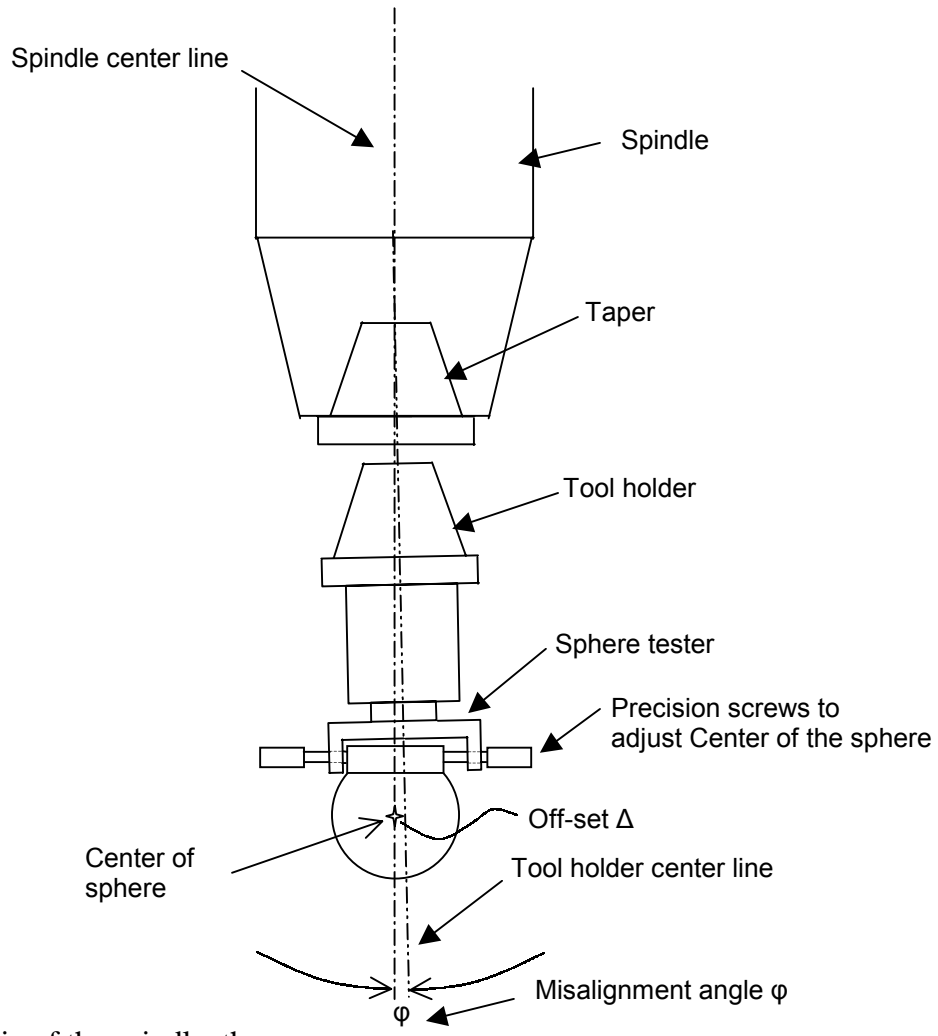


Fig. 3 A schematic of the spindle, the tool holder, and the sphere tester

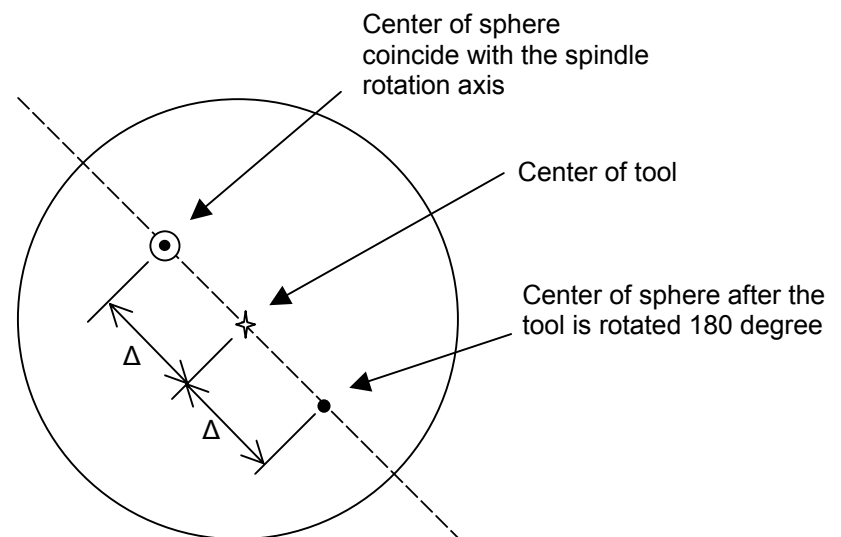


Fig.4 A schematic illustrate the effect of rotating the tool holder by 180 degree

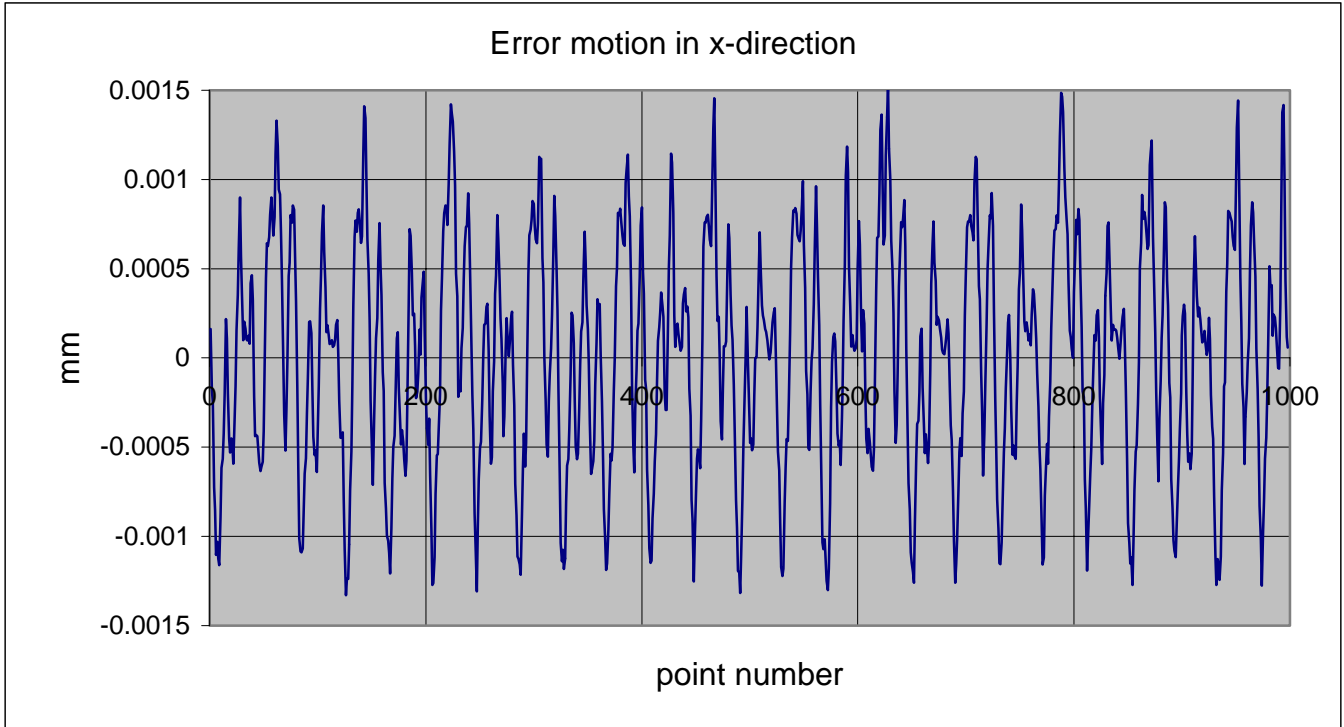


Fig. 5 Spindle error motion measured in x-direction

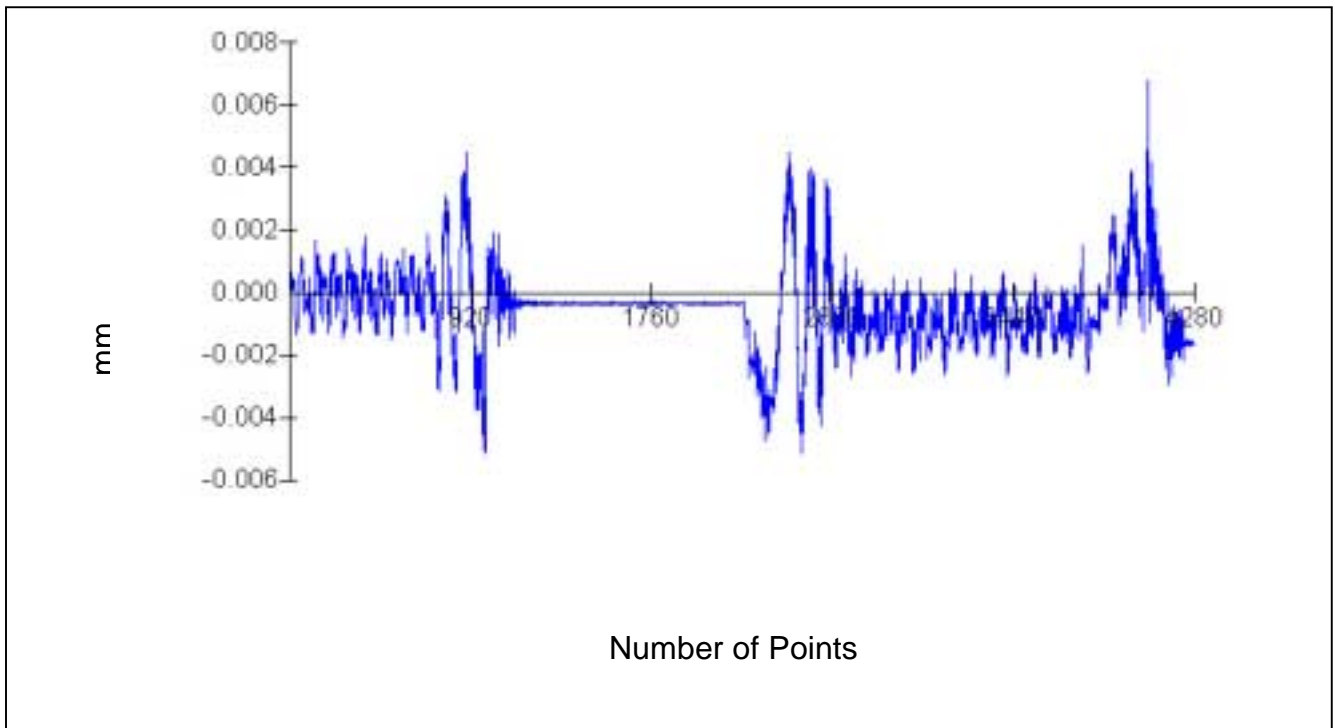


Fig. 6 Spindle error motion measured in x-direction at 800 rpm with start and stop

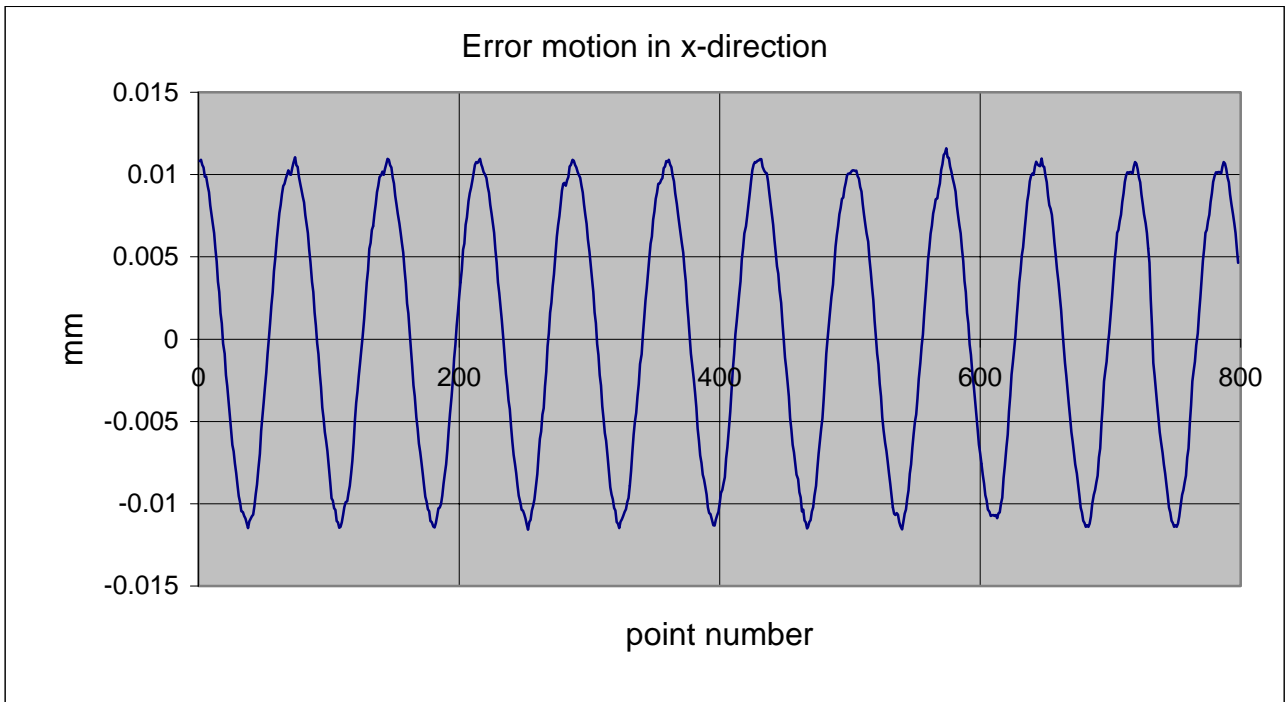


Fig. 7a Spindle error motion measured in x-direction after the tool holder was rotated 180 degree

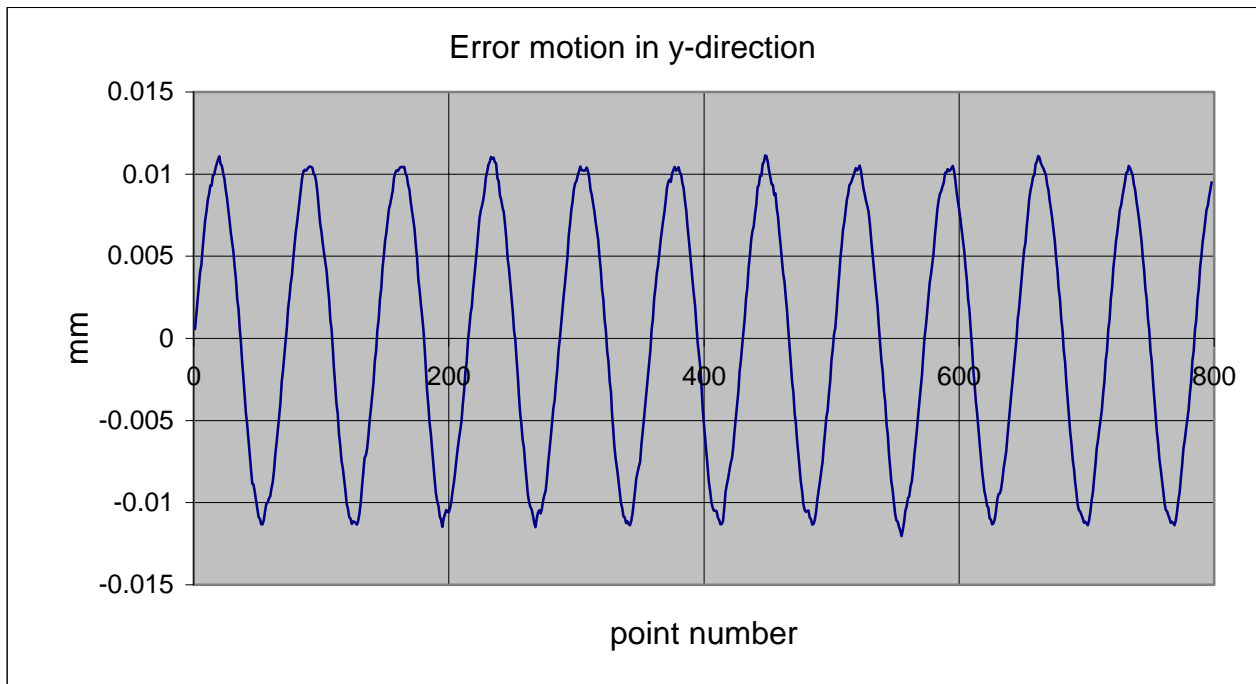


Fig. 7b Spindle error motion measured in y-direction after the tool holder was rotated 180 degree

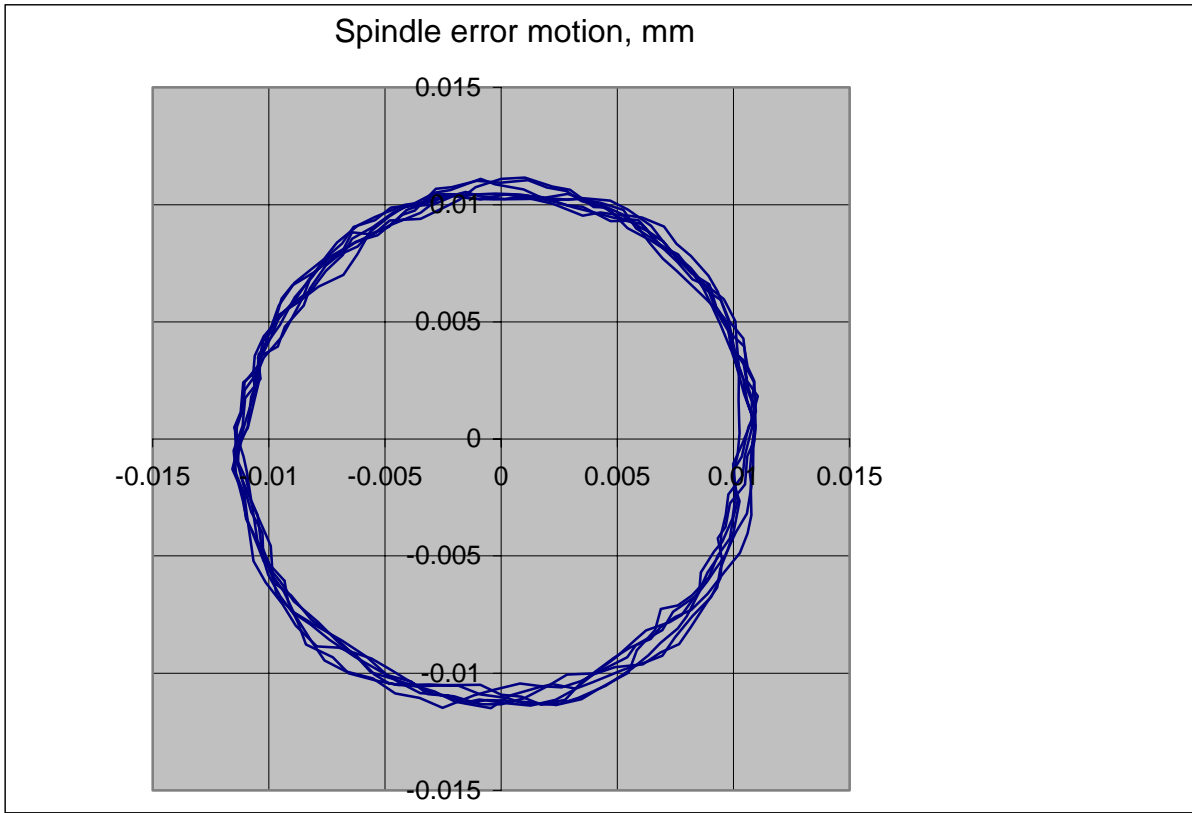


Fig. 8 A polar plot of the radial error motion after the tool holder was rotated 180 degree

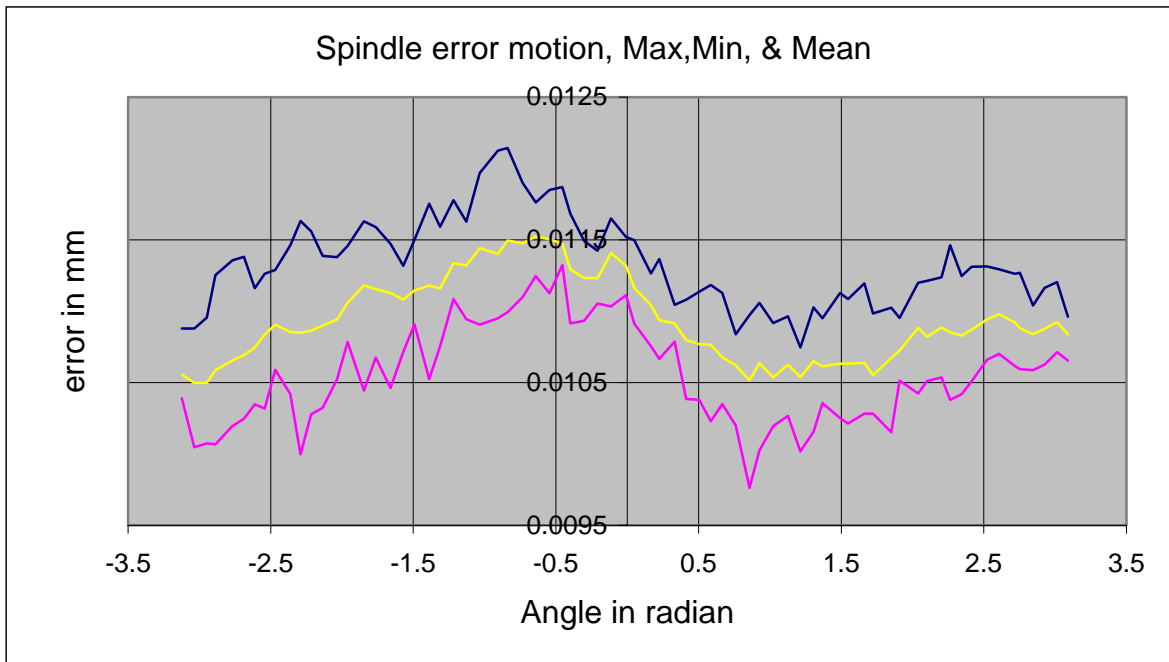


Fig. 9 A plot of the average, maximum and minimum error motion

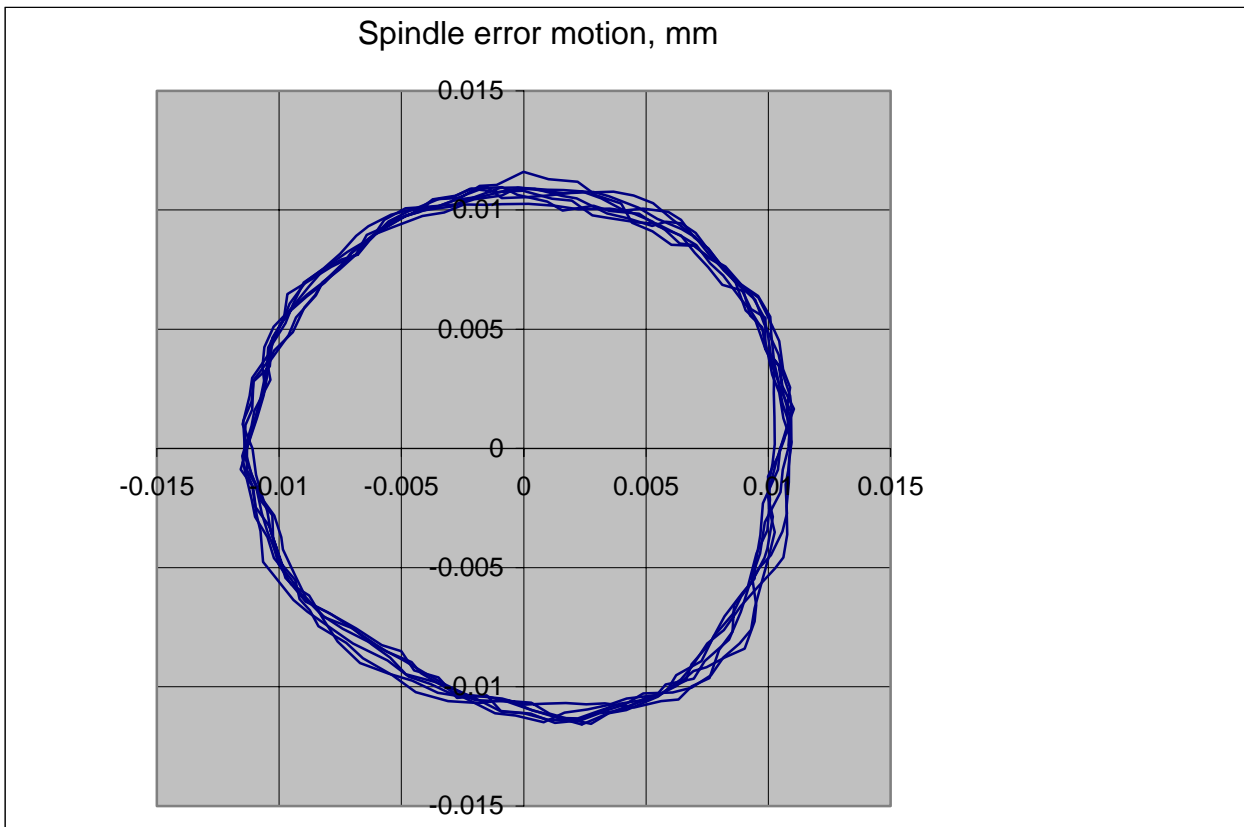


Fig. 10 A polar plot using the measurement in the x-direction and shifted 90 degrees for the y-direction

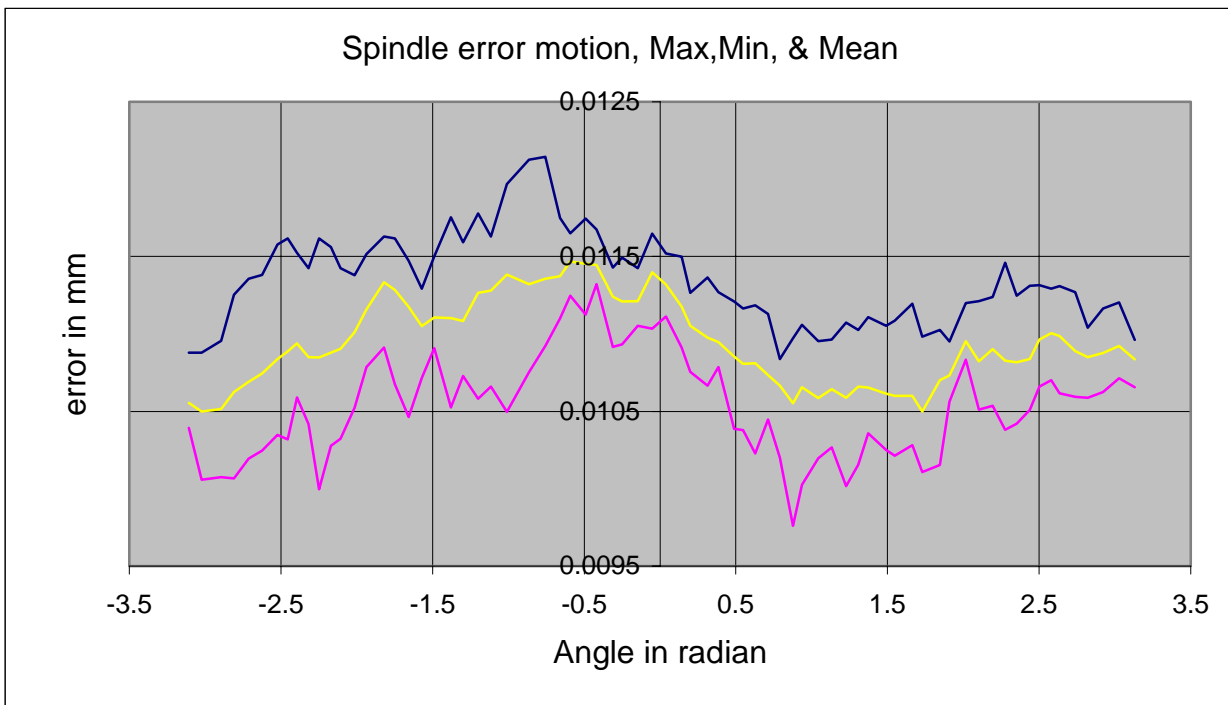


Fig. 11 A plot of the average, maximum and minimum error motion using the measurement in the x-direction and shifted 90 degrees for the y-direction